potential coulometry experiments show that a total of two electrons are consumed in the net defluorination of CF_3Cba's, we propose the ECE mechanism shown in Scheme II.[37] Here, the anticipated one-electron reduction leads to the radical anion **3**, which partitions between carbon–cobalt bond cleavage and elimination of fluorine to form the radical intermediate **4**. The latter then undergoes an additional one-electron reduction to form the anion **5**, the analogue of species **2** (Scheme I) proposed as the intermediate in the reductive dehalogenation of α-(haloalkyl)cobaloximes by Ricroch et al.[2] This species may be described as the cobalt(II)–difluorocarbenoid species **5b** or the equivalent valence-bond structures **5a** and **5c**. As in the case of the cobaloximes, protonation of this species leads to the difluorocobamide.

Evidence for the partitioning of the radical anion **3** between carbon–cobalt bond homolysis and defluorination comes from the observation that controlled-potential reduction of β-CF_3Cbl in DMF/1-propanol yields dealkylation only: no β-CF_2HCbl could be detected. In this solvent, which provides ample abstractable hydrogen atoms, the dealkylation of $CH_3Cbl^{\bullet-}$ and $CH_3Cbi^{\bullet-}$ is known to be extremely rapid,[24] while, in water, carbon–cobalt bond cleavage of base-off $CH_3Cbl^{\bullet-}$ is reported[23] to occur at a rate comparable to those observed here for defluorination of the CF_3Cba's. Direct evidence that solvent is the source of the CF_2H proton comes from the observation of formation of the CF_2DCbl's in deuterated media. Surprisingly, the opposite result was obtained when β-CF_3Cbl was defluorinated by borohydride, β-CF_2DCbl being obtained with $NaBD_4/H_2O$, while β-CF_2HCbl was the product in $NaBH_4/D_2O$. This indicates that reductive defluorination of CF_3Cba's with BH_4^- occurs by a different mechanism than that operative with zinc reductants and controlled-potential reduction. As this result is also opposite to that of Ricroch et al.[2] for the reductive dehalogenation of α-(haloalkyl)cobaloximes by BH_4^-, the mechanism of reductive dehalogenation of α-(haloalkyl)cobaloximes by BH_4^- is also different from that of CF_3Cba defluorination by BH_4^-. Our observations suggest that the latter reaction may result from the direct attack of a hydride ion on the α-carbon of the CF_3Cba.

While β-CF_3Cbl was found to be slowly dealkylated ($t_{1/2} > 2$ h) by Ti(III), no defluorination was observed under conditions similar to those employed by Hogenkamp et al.[12] for the reductive dehalogenation of CF_3Cl by Ti(III) catalyzed by cobamides. This observation supports the conclusion of these workers that the cobamide-catalyzed dehalogenation of CF_3Cl by Ti(III) occurs by reductive dealkylation of CF_3Cba's followed by further reaction of $CF_3^{\bullet}$ and not by defluorination of CF_3Cba's.

In sum, reductive defluorination of CF_3Cba's by zinc reductants and controlled-potential reduction appear to occur by the ECE mechanism of Scheme II, but by a different mechanism when $NaBH_4^-$ is the reductant. Several interesting differences in the behavior of cobaloximes and cobamides in this regard have been revealed. Thus, (trifluoromethyl)cobaloximes are stable to reduction by zinc[5] but defluorinated by borohydride,[3,8] presumably by a mechanism in which the CF_2H proton comes from solvent.[3] In contrast, (trifluoromethyl)cobamides are defluorinated by zinc (and controlled-potential reduction), apparently by the ECE mechanism of Scheme II, in which the CF_2H proton comes from solvent, but are defluorinated by borohydride by a different mechanism in which the CF_2H proton comes from the reductant.

(37) A reviewer has pointed out that the current data do not eliminate the possibility that the dealkylation step is heterolytic, i.e., $[CF_3\text{–}Co^{III}]^{\bullet-} \rightarrow Co^{II} + CF_3^-$. However, the complete suppression of defluorination in DMF/1-propanol suggests the homolysis mechanism depicted in Scheme II. See also the arguments of Zhou et al.[26]

Acknowledgment. This research was supported by the National Science Foundation (Grants CHE 89-96104 and RII-89-02064), the State of Mississippi, and Mississippi State University.

Contribution from the Department of Chemistry, Purdue University, West Lafayette, Indiana 47907

Non-Metal Redox Kinetics: Iodine Monobromide Reaction with Iodide Ion and the Hydrolysis of IBr

Robert C. Troy,† Mark D. Kelley, Julius C. Nagy, and Dale W. Margerum*

Received June 16, 1991

The dissociation equilibrium constant for IBr_2^-, $K_1 = (3.5 \pm 0.6) \times 10^{-3}$ M at 25.0 °C and $\mu = 1.0$ M, is determined. Pulsed-accelerated-flow (PAF) methods are used to measure the very rapid reactions when solutions of IBr_2^-/Br^- are mixed with excess I^- in 1.0 M H^+ at 25.0 °C. The proposed mechanism is as follows:

$$IBr_2^- \underset{k_{-1}}{\overset{k_1}{\rightleftharpoons}} IBr(aq) + Br^-$$

$$IBr(aq) + I^- \underset{k_{-2}}{\overset{k_2}{\rightleftharpoons}} I_2Br^-$$

$$I_2Br^- \underset{k_{-3}}{\overset{k_3}{\rightleftharpoons}} I_2(aq) + Br^-$$

$$I_2(aq) + I^- \underset{k_{-4}}{\overset{k_4}{\rightleftharpoons}} I_3^-$$

Reactant concentrations are adjusted so that I_2Br^- formation is the rate-determining step; k_2 is $(2.0 \pm 0.3) \times 10^9$ M^{-1} s^{-1} and k_{-2} is 800 ± 300 s^{-1} (from studies under reversible conditions). The k_2 rate constant is intermediate between values of the rate constants for I^- with ICl(aq) and I^- with I_2(aq). The equilibrium constant for the hydrolysis of IBr(aq) is $(2.4 \pm 0.4) \times 10^{-7}$ M^2 at 25.0 °C, $\mu = 0.5$ M, for $IBr(aq) + H_2O \rightleftarrows HOI + Br^- + H^+$. PAF methods are used to study the reactions of IBr_2^-/Br^- solutions with bases. The hydrolysis of IBr(aq) is extremely rapid; $k_{hydr} = k_{H_2O} + k_{OH}[OH^-] + k_B[B]$, where $k_{H_2O} = (8 \pm 3) \times 10^5$ s^{-1}, $k_{OH} = (6.0 \pm 0.4) \times 10^9$ M^{-1} s^{-1}, and $k_B = (3.5 \pm 0.2) \times 10^9$ M^{-1} s^{-1} for $B = CO_3^{2-}$ or PO_4^{3-}. Two IBr(aq) species are proposed to be in rapid equilibrium: H_2OIBr (50%) and IBr (50%), where the less hydrated IBr species reacts with PO_4^{3-} and CO_3^{2-} at the diffusion limit.

Introduction

Hydrolysis reactions of diatomic interhalogen compounds of iodine, bromine, and chlorine are extremely rapid compared to reactions of the halogens themselves.[1,2] The rate constant for the hydrolysis of ICl(aq)[1] is 2.4×10^6 s^{-1} compared to values of

† Present address: State University of New York, Purchase.

(1) Wang, Y. L.; Nagy, J. C.; Margerum, D. W. *J. Am. Chem. Soc.* **1989**, *111*, 7838-7844.

0020-1669/91/1330-4838$02.50/0

Table I. Equilibrium Constants for Iodine–Bromine Species in Aqueous Solution[a]

reaction	equilib const	ref
$IBr_2^- \rightleftharpoons IBr(aq) + Br^-$	$K_1 = 0.0035$ M	*b*
$IBr(aq) + I^- \rightleftharpoons I_2Br^-$	$K_2 = 2 \times 10^6$ M^{-1}	12[c]
$I_2Br^- \rightleftharpoons I_2(aq) + Br^-$	$K_3 = 0.079$ M	10
$I_2(aq) + I^- \rightleftharpoons I_3^-$	$K_4 = 721$ M^{-1}	11
$IBr(aq) + H_2O \rightleftharpoons HOI + H^+ + Br^-$	$K_5 = 2.4 \times 10^{-7}$ M^2	*b*, *d*

[a] Conditions: $\mu = 1.0$ M, 25.0 °C. [b] This work. [c] The value is corrected with above values of K_1 and K_3. [d] $\mu = 0.50$ M.

3.0 s^{-1} for $I_2(aq)$ and 11.0 s^{-1} for $Cl_2(aq)$.[2] Iodine monobromide is a well-known compound that hydrolyzes rapidly in water.[3] The hydrolysis rate constant of IBr(aq) has been estimated in fitting oscillating reaction mechanisms for the bromate–iodide system[4] and for the bromate–chlorite–iodide system.[5] These indirect estimates gave an initial value[4] of 30 s^{-1} and a revised value[5] of 1.5×10^3 s^{-1}. The present work uses the pulsed-accelerated-flow (PAF) method[6,7] to study the rates of hydrolysis of IBr(aq) with water and with bases. This shows that both of the previous estimates for the hydrolysis rate constant are several orders of magnitude too small.

In recent studies[8] of the reactions between OBr^-/HOBr and I^-, IBr(aq) is proposed as an intermediate. Its subsequent rates of reaction with I^-, H_2O, and OH^- are important in the evaluation of these reaction mechanisms. Dibromoiodate(I) ion, IBr_2^-, is a convenient source of iodine monobromide (eq 1) for studies of

$$IBr_2^- \rightleftarrows IBr(aq) + Br^- \quad K_1 \tag{1}$$

the reactivity of IBr(aq). Its reaction with I^- (eq 2) is too fast

$$IBr(aq) + I^- \rightleftarrows I_2Br^- \quad K_2 \tag{2}$$

to measure by stopped-flow spectroscopy but can be measured by the PAF method. The techniques are similar to those used in the studies of ICl(aq),[1,9] where ICl_2^- in the presence of excess Cl^- (in order to suppress the rates) was reacted with base or with I^-. In the reaction of IBr_2^- with I^-, the concentrations of I^- and Br^- determine the observed rate constants and the final mixtures of products (eqs 3 and 4),[10,11] provided the H^+ and Br^- concentrations are sufficient to prevent the hydrolysis reaction in eq 5.

$$I_2Br^- \rightleftarrows I_2(aq) + Br^- \quad K_3 \tag{3}$$

$$I_2(aq) + I^- \rightleftarrows I_3^- \quad K_4 \tag{4}$$

$$IBr(aq) + H_2O \rightleftarrows HOI + H^+ + Br^- \quad K_5 \tag{5}$$

The UV–vis spectral characteristics of I_2Br^- in aqueous solution are reported in this work because there has been insufficient information about its absorption peaks and molar absorptivity values.

The IBr_2^-/IBr(aq) system and PAF techniques are also used to measure the very fast reactions of OH^-, PO_4^{3-}, CO_3^{2-}, and H_2O with IBr(aq).

New values for the equilibrium constants in eqs 1 and 5 are measured. Table I gives these values and the equilibrium constants for eqs 2–4.[10-12]

Table II. Spectral Characteristics of Iodine–Bromine and Iodine Species in Aqueous Solution

species	λ_{max}, nm (ϵ, M^{-1} cm^{-1})[a]	ϵ,[a] M^{-1} cm^{-1}	
		λ = 428 nm	λ = 440 nm
I_2	460 (750)	530	650
	207 (20000)		
I_3^-	351 (27000)	2500	1800
	288 (40000)		
IBr_2^-	375 (580)	140	97
	253 (55000)		
I_2Br^-	273 (61000)	3000	2700
	350 (13000)[b]		
IBr(aq)	375 (370 ± 30)[c]		

[a] Average precision is ≤ 3%. [b] Absorbance shoulder. [c] Not λ_{max}.

Experimental Section

Solutions of $HClO_4$ and HBr were standardized with NaOH, which in turn was standardized against potassium hydrogen phthalate with phenolphthalein indicator. All HBr solutions were checked before use to be sure there was no Br_3^- contamination (λ = 266 nm, ϵ = 35000 M^{-1} cm^{-1}).[13] Solutions of NaI were standardized by using bromine oxidation to convert iodide to iodate and then by iodometric titrations with standardized $Na_2S_2O_3$.[14] The stock NaI solution (pH 7) was purged with Ar (to prevent oxidation of iodide by dissolved oxygen) and stored in the dark. Iodide solutions used for kinetics studies were made by dilution of the stock NaI solution immediately before use. Solutions of iodine (used for spectroscopic studies) were prepared by washing solid I_2 (Mallinckrodt, resublimed) in approximately 1 mM $HClO_4$ solution several times. The washed solid was dissolved in 1 mM $HClO_4$ to prevent hydrolysis of I_2 to HOI.

Buffer solutions were prepared from NaH_2PO_4/Na_2HPO_4, Na_2HPO_4/Na_3PO_4, and $NaHCO_3/Na_2CO_3$ mixtures. The pK_a values (25.0 °C, μ = 0.50 M) are 6.46[15] for $H_2PO_4^-$, 11.34[16] for HPO_4^-, and 9.70[17,18] for HCO_3^-. The pK_w value is 13.72.[19]

A 0.11 M stock solution of IBr_2^- was prepared by adding NaI to a solution of primary standard grade $NaIO_3$ in 0.9 M HBr by a method analogous to the preparation of ICl_2^- in solution.[20] Two moles of NaI were added for each mole of $NaIO_3$ (eq 6). The IBr_2^- concentration was

$$IO_3^- + 2I^- + 6Br^- + 6H^+ \rightarrow 3IBr_2^- + 3H_2O \tag{6}$$

determined spectrophotometrically at 375 nm with the values given in Table II. Spectral results were recorded with a Perkin-Elmer Model 320 UV–visible spectrophotometer interfaced to a Perkin-Elmer 3600 data station. All scans were done at 25.0 ± 0.2 °C.

The equilibrium constant (K_1) for the reaction given in eq 1 was determined spectrophotometrically at 25.0 °C, μ = 1.0 M. A stock solution of 0.11 M IBr_2^- in 0.69 M HBr was diluted 100-fold in 1.0 M $HClO_4$. An aliquot (2.50 mL) of the diluted solution was placed in a 1.00 cm quartz cell, and small aliquots (0.0100 mL) of 1.0 M HBr were added. After each addition of HBr solution, the absorbance (375 nm) of the resulting solution was recorded. A nonlinear curve-fitting procedure,[1] based on the Marquardt algorithm,[21] was used to fit the absorbance vs $[Br^-]$. The $[Br^-]$ comes from three sources: the original [HBr] in the stock ($[Br^-]_i$), the [HBr] added ($[Br^-]_a$), and the amount dissociated from the IBr_2^- equilibrium ($[Br^-]_d$). $[Br^-]_d$ is dependent on K_1, and therefore an iterative process is used to give $[Br^-]$. The relationship between the observed absorbance (after correction for dilution, 1.00-cm cell) and the concentrations of absorbing species is given in eq 7 where

$$A_{375} = \frac{[IBr]_T ([Br^-]_T \epsilon_{IBr_2} + K_1 \epsilon_{IBr})}{K_1 + [Br^-]_T} \tag{7}$$

$[IBr]_T = [IBr_2^-] + [IBr(aq)]$, $[Br^-]_T = [Br^-]_i + [Br^-]_a + [Br^-]_d$, and ϵ = molar absorptivity (M^{-1} cm^{-1}) of the respective species.

(2) Eigen, M.; Kustin, K. *J. Am. Chem. Soc.* **1962**, *84*, 1355–1361.
(3) Faull, J. H. *J. Am. Chem. Soc.* **1934**, *56*, 522–526.
(4) Citri, O.; Epstein, I. R. *J. Am. Chem. Soc.* **1986**, *108*, 357–363.
(5) Citri, O.; Epstein, I. R. *J. Phys. Chem.* **1988**, *92*, 1865–1871.
(6) Jacobs, S. A.; Nemeth, M. T.; Kramer, G. W.; Ridley, T. Y.; Margerum, D. W. *Anal. Chem.* **1984**, *56*, 1058–1065.
(7) Nemeth, M. T.; Fogelman, K. D.; Ridley, T. Y.; Margerum, D. W. *Anal. Chem.* **1987**, *59*, 283–291.
(8) Troy, R. C.; Margerum, D. W. *Inorg. Chem.* **1991**, *30*, 3538–3543.
(9) Margerum, D. W.; Dickson, P. N.; Nagy, J. C.; Kumar, K.; Bowers, C. P.; Fogelman, K. D. *Inorg. Chem.* **1986**, *25*, 4900–4904.
(10) La Mer, V. K.; Lewinsohn, M. H. *J. Phys. Chem.* **1934**, *38*, 171–195.
(11) Ramette, R. W.; Sanford, R. W. *J. Am. Chem. Soc.* **1965**, *87*, 5001–5005. Turner, D. H.; Flynn, G. W.; Sutin, N.; Beitz, J. V. *J. Am. Chem. Soc.* **1972**, *94*, 1554–1559. Daniele, G. *Gazz. Chim. Ital.* **1960**, *90*, 1068–1081. Katzin, L. I.; Gerbert, E. J. *J. Am. Chem. Soc.* **1955**, *77*, 5814–5819.
(12) Gilbert, F. L.; Goldstein, R. R.; Lowry, T. M. *J. Chem. Soc.* **1931**, *134*, 1092–1103.
(13) Soulard, M.; Block, F.; Hatterer, A. *J. Chem. Soc., Dalton Trans.* **1981**, 2300–2310.
(14) Koltoff, I. M.; Sandell, E. B.; Meehan, E. J.; Bruckenstein, S. *Quantitative Chemical Analysis*, 4th ed.; Macmillan: London, 1969; p 852.
(15) Mesmer, R. E.; Baes, C. F. *J. Solution Chem.* **1974**, *3*, 307–321.
(16) Hitch, B. F.; Mesmer, R. E. *J. Solution Chem.* **1976**, *5*, 667–680.
(17) Fogelman, K. D.; Walker, D. M.; Margerum, D. W. *Inorg. Chem.* **1989**, *28*, 986–993.
(18) Odier, M.; Plichon, V. *Anal. Chim. Acta* **1971**, *55*, 209–220.
(19) Sweeton, F. H.; Mesmer, R. E.; Baes, C. F. *J. Solution Chem.* **1974**, *3*, 191–214.
(20) Philbrick, F. A. *J. Chem. Soc.* **1930**, 2254–2260.
(21) Bevington, P. R. *Data Reduction and Error Analysis for the Physical Sciences*, McGraw-Hill: New York, 1969, pp 235–240.

Pulsed-Accelerated-Flow Method. The PAF Model IV spectrometer[17,22] was used to obtain kinetic data for the reactions of iodide with IBr. This instrument has a wavelength range of 200–850 nm and a double monochromator that gives much higher light throughput as compared with earlier models.[6,7] The PAF spectrometer employs integrating observation[23,24] during continuous-flow mixing of short duration (a 0.4-s pulse). The purpose of the pulsed flow is to conserve reagents.[6,7] The reactants are observed along the direction of flow from their point of mixing to their exit from the observation tube (1.025 cm). A twin-path mixing/observation cell made from polyvinyl chloride is used.[7] In this study, the flow was decelerated during the pulse to give a linear velocity ramp, and 250 measurements of the transmittance were taken as the flow velocity in the observation tube changed from 12.5 to 3.0 m s^{-1}. The velocity variation permits the chemical-reaction-rate process to be resolved from the mixing-rate process.[6,7] The method of observation, the efficient mixing, and the variation of flow velocity permit accurate measurement of first-order rate constants as much as a factor of 10^3 larger than can be measured by typical stopped-flow methods. Solution reservoirs, drive syringes, and the mixing/observation cell were thermostated at 25.0 ± 0.2 °C with a circulating water bath. Reactant solutions were drawn directly from the reservoirs into the drive syringes through Teflon tubing.

The fundamental relationship used in the analysis of first-order PAF data is given in eq 8, where M_{exp} is the defined absorbance ratio, A_v is

$$M_{exp} = \frac{A_v - A_\infty}{A_0 - A_\infty} = \frac{1 - e^{-Y}}{Y} \qquad Y = \frac{bk_{app}}{v} \tag{8}$$

the absorbance of the reaction mixture at a given instantaneous velocity, A_∞ is the absorbance at infinite time, A_0 is the absorbance at time zero, k_{app} is the apparent rate constant (s^{-1}), b is the reaction path length (=0.01025 m), v is the solution velocity in the observation tube (m s^{-1}), and Y is a parameter which is iterated to fit the equation.[23,24] All absorbances are measured in the PAF spectrometer. The apparent rate constant, k_{app}, is related to the reaction rate constant, k_r (s^{-1}), and a mixing rate constant, k_{mix} (s^{-1}), by eq 9.[6,7] The mixing rate constant,

$$\frac{1}{k_{app}} = \frac{1}{k_{mix}} + \frac{1}{k_r} \tag{9}$$

k_{mix}, depends on the velocity (eq 10), where k_m is a mixing constant.

$$k_{mix} = k_m v \tag{10}$$

Typically, k_m is greater than 1700 m^{-1} and v is 3.0 to 12.5 m s^{-1}. For first-order rate constants greater than 4000 s^{-1}, $\exp(-Y) \ll 1$ in eq 8, and the model simplifies to eq 11. Substitution of eqs 9 and 10 into eq 11

$$M_{exp} = \frac{A_v - A_\infty}{A_0 - A_\infty} = \frac{1}{Y} = \frac{v}{bk_{app}} \tag{11}$$

yields eq 12, where M_{exp} is a linear function of velocity for fast reactions.

$$M_{exp} = \frac{A_v - A_\infty}{A_0 - A_\infty} = \frac{1}{bk_m} + \frac{v}{bk_r} \tag{12}$$

Plots of M_{exp} vs v have slopes of $1/(bk_r)$ and intercepts of $1/(bk_m)$ for first-order reactions. Pseudo-first-order rate constants (k_r) greater than 4000 s^{-1} reported in this work for the IBr(aq) with I^- reaction are obtained from linear regressions of M_{exp} vs v plots as given in eq 12. For those below 4000 s^{-1}, a double-reciprocal plot of $1/k_{app}$ vs $1/v$ was used according to eqs 8 and 9.

PAF kinetic data for the IBr(aq) reaction with I^- (μ = 1.0 M ([$HClO_4$] + [HBr]) and 25.0 °C) are obtained by following the appearance of I_2Br^- at 428 or 440 nm or the appearance of I_3^- at 353 nm. When I^- concentrations greater than 1 mM are mixed with the corresponding $HClO_4$/HBr solutions without I^-, a small absorbance contribution occurs during mixing because of the refractive index differences of the solutions. This absorbance is due to light scattering, and it decreases as the velocity increases, because k_{mix} increases with velocity.[25] These absorbance vs velocity data are subtracted from the reaction absorbance data before the usual analysis.

For the IBr(aq) hydrolysis reactions, the kinetic data are analyzed by eq 12 for smaller rate constants and by eq 13 for larger rate constants.

$$M_{exp} = \frac{1}{bk_m} + \frac{v}{bk_r} + \frac{c}{v} \tag{13}$$

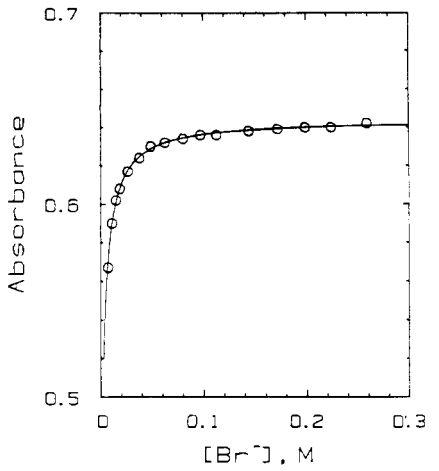

Figure 1. Spectrophotometric data for measurement of K_1 in 1.0 M $HClO_4$ ($[IBr]_T = 1.1 \times 10^{-3}$ M; λ = 375 nm; 1.00-cm cell; 25.0 ± 0.2 °C). The solid line shows the fit of eq 7 for $K_1 = 3.5 \times 10^{-3}$.

The c/v term is necessary when the extent of reaction in the center of the mixing cell becomes appreciable (when the value of k_r is greater than 60 000 s^{-1}).[22] All kinetic data are collected at μ = 0.50 M (NaBr) and 25.0 °C by following the disappearance of IBr_2^- at 253 nm.

The k_r values reported in the tables are averages of at least three trials. The values in parentheses denote 1 standard deviation in the last digit.

Results and Discussion

Equilibrium Constant for $IBr_2^- \rightleftarrows IBr(aq) + Br^-$. A K_1 value of (3.5 ± 0.6) × 10^{-3} M (25.0 °C in 1.0 M $HClO_4$) is determined from spectrophotometric measurements. Figure 1 shows the absorbance (375 nm) vs. $[Br^-]_T$ data as fitted to eq 7. From this procedure, the molar absorptivities (M^{-1} cm^{-1}) at 375 nm are 580 ± 1 for IBr_2^- and 370 ± 30 for IBr(aq). Under the conditions used, the concentrations of HOI and H_2OI^+ are negligible and need not be considered[1] in the evaluation of K_1. The value for ϵ_{IBr_2} is in good agreement with previous reports.[26,27] Our value for ϵ_{IBr} is similar to the value of 360 M^{-1} cm^{-1} at 375 nm measured in ethyl acetate.[28] King and Lister[26] reported ϵ_{IBr} = 310 M^{-1} cm^{-1} at 380 nm in aqueous solution, but their calculations for the IBr(aq) concentration were based on Faull's[3] average value of K_1. This equilibrium constant was determined by extraction equilibration methods. Faull reported a K_1 value of 0.0027 M that was obtained from the average of a series of values measured at different ionic strengths (μ = 0.10–1.0 M). His K_1 value for μ = 1.0 M was 0.0033 M, which is in excellent agreement with our results. Appelman[29] reported a K_1 value of 0.0022 M at 20 °C. Eyal and Treinin[30] showed that the K_1 value is temperature sensitive. Their spectrophotometric method gave a K_1 value of 0.003 M at 25 °C, μ = 0.02 M ($HClO_4$). Thus, the equilibrium constants are in general agreement for the same temperature and ionic strength conditions.

UV–Vis Spectral Characteristics of I_2Br^-. Figures 2 and 3 show the absorption spectra over two wavelength regions for IBr_2^- and for I_2Br^-. There is lack of agreement about the nature of the aqueous I_2Br^- spectrum. We find two shoulders at 350 and 428 nm as well as a peak at 273 nm. A previous report[31] claimed that the band above 400 nm is due to a shifted I_2 peak in Br^- medium, but we assign this band to I_2Br^-. This polyhalide ion has a linear structure in its $Cs(I_2Br)$ salt[32] with I–I and I–Br bond lengths of 2.78 and 2.91 Å, respectively.

A solution with I_2Br^- as one of the main species was prepared with initial concentrations of 1.0 × 10^{-5} M I_2, 0.20 M Br^-, and

(22) Bowers, C. P.; Fogelman, K. D.; Nagy, J. C.; Ridley, T. Y.; Wang, Y. L.; Margerum, D. W. To be submitted for publication.
(23) Gerischer, H.; Heim, W. *Z. Phys. Chem. (Munich)* **1965**, *46*, 345–352.
(24) Gerischer, H.; Heim, W. *Ber. Bunsen-Ges. Phys. Chem.* **1967**, *71*, 1040–1046.
(25) Dickson, P. N. Ph.D. Thesis, Purdue University, 1986.
(26) King, D. E.; Lister, M. W. *Can. J. Chem.* **1968**, *46*, 279–286.
(27) Mills, J. F. In *Disinfection Water and Wastewater*; Johnson, J. D., Ed.; Ann Arbor Science: Ann Arbor, MI, 1975; p 113.
(28) Gillam, A. E. *Trans. Faraday Soc.* **1933**, 1132–1139.
(29) Appelman, E. H. *J. Phys. Chem.* **1961**, *65*, 325–331.
(30) Eyal, E.; Treinin, A. *J. Am. Chem. Soc.* **1964**, *86*, 4287–4290.
(31) Savko, S. S.; Faerman, G. P. *Opt. Spektrosk.* **1966**, *21*, 763–766.
(32) Migchelsen, L.; Vos, A. *Acta Crystallogr.* **1967**, *22*, 812–815.

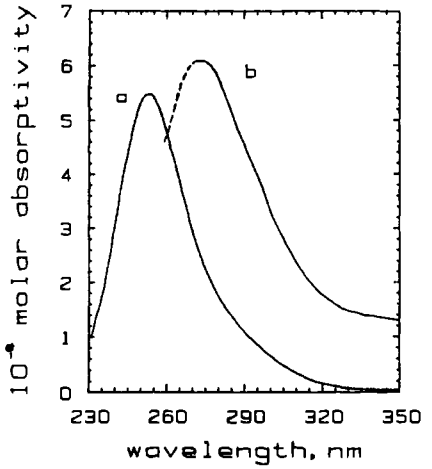

Figure 2. Ultraviolet absorption spectra of IBr_2^- (a) and I_2Br^- (b). (The dashed line indicates regions where the errors in ϵ may exceed 20%.)

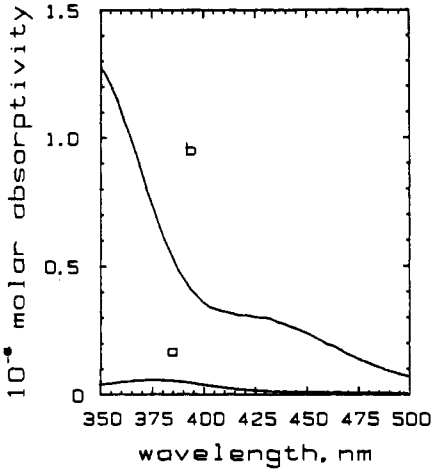

Figure 3. Visible absorption spectra for IBr_2^- (a) and I_2Br^- (b).

1.0×10^{-3} M I^-. A COMICS program[33] was used with the equilibrium constants given in Table I to calculate the species distribution of $I_2(aq)$, I_2Br^-, IBr_2^-, IBr(aq), and I_3^-. The equilibrium concentrations (M) were as follows: $[I_2Br^-] = 5.7 \times 10^{-6}$; $[I_2(aq)] = 2.4 \times 10^{-6}$; $[I_3^-] = 1.8 \times 10^{-6}$; $[IBr_2^-] = 1.1 \times 10^{-9}$; $[IBr(aq)] = 1.9 \times 10^{-9}$. In separate experiments we measured the spectra of $I_2(aq)$, I_3^-, and IBr_2^- (Table II) and obtained results in excellent agreement with known values.[26,27,34,35] The absorbances due to each of these species are subtracted from the experimental spectrum to give the corrected I_2Br^- spectrum in Figures 2 and 3 and the molar absorptivity values in Table II.

Studies of the spectra of polyhalide salts in nonaqueous solvents[12,36] are in general agreement with our results. For example, $(CH_3)_4NI_2Br$ in acetonitrile has bands at 351 nm (ϵ = 11 600 M^{-1} cm^{-1}) and 280 nm (ϵ = 40 600 M^{-1} cm^{-1}) compared to our values in aqueous solution of 350 nm (ϵ = 13 000 M^{-1} cm^{-1}) and 273 nm (ϵ = 61 000 M^{-1} cm^{-1}). Another report[30] gives λ_{max} at 270 nm (ϵ = 55 000 M^{-1} cm^{-1}) for the aqueous I_2Br^- spectrum.

Kinetics of the IBr(aq) + I^- ⇄ I_2Br^-(aq) Reaction. Dilute solutions of IBr_2^- (1.0×10^{-5} M) in the presence of high concentrations of Br^- (0.60–1.00 M) with moderate I^- concentrations (0.2–1.0 mM) are mixed so that the primary reactants and products are given by eq 14. This gives pseudo-first-order reversible kinetics. The reaction rate is proportional to the I^- concentration and is inversely proportional to the Br^- concentration.

$$IBr_2^- + I^- \rightleftarrows I_2Br^- + Br^- \qquad (14)$$

(33) Perrin, D. D.; Sayce, I. G. *Talanta* **1967**, *14*, 833–842.
(34) Crouse, W. C.; Margerum, D. W. *Inorg. Chem.* **1974**, *13*, 1437–1443.
(35) Awtrey, A. D.; Connick, R. E. *J. Am. Chem. Soc.* **1951**, *73*, 1842–1843.
(36) Popov, A. I.; Swenson, R. F. *J. Am. Chem. Soc.* **1955**, *77*, 3724–3726.

Table III. Pseudo-First-Order Rate Constants for the Reaction of IBr_2^- with I^- [a,b]

$[Br^-]$, M	$10^3[I^-]$, M	$10^{-3}k_r$, s^{-1}
1.00	0.20	2.11 (5)
1.00	0.40	3.59 (9)
1.00	0.60	5.32 (3)
1.00	0.80	6.7 (8)
1.00	1.0	7.4 (3)
1.00	1.00	8.6 (9)[c]
1.00	1.25	10.6 (7)[c]
1.00	1.50	12.2 (8)[c]
0.80	0.193	2.25 (3)
0.80	0.362	3.58 (3)
0.80	0.483	4.67 (7)
0.80	0.724	6.9 (3)
0.80	0.996	9.3 (3)
0.60	0.181	2.92 (4)
0.60	0.272	3.95 (7)
0.60	0.363	5.32 (6)
0.60	0.453	6.2 (1)
0.60	0.544	7.2 (1)
0.10	0.250	15.6 (4)[c]
0.10	0.375	23.8 (2)[c]
0.10	0.500	33.8 (5)[c]
0.10	0.625	41.4 (7)[c]

[a] $[IBr]_T = 1.0 \times 10^{-5}$ M, 1.0 M $[H^+]$, μ = 1.0 M, 25.0 °C. [b] 0.80 M and 0.60 M Br^- data at 428 nm; 1.0 M Br^- data at 440 nm. [c] Appearance of I_3^- measured at 353 nm.

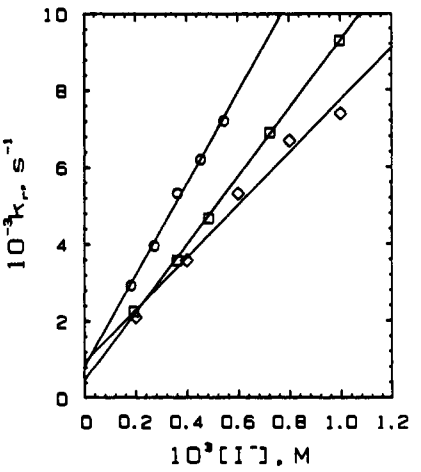

Figure 4. Pseudo-first-order rate constants (25.0 °C) vs $[I^-]$ for the reaction of IBr + I^- in 1.0 M H^+. $[Br^-]$ = (○) 0.60, (□) 0.80, and (◇) 1.0 M ($[IBr]_T = 1.0 \times 10^{-5}$ M; λ = 428 nm for ○ and □ and 440 nm for ◇).

This indicates that I^- does not react directly with IBr_2^-, but instead reacts with IBr(aq).

The reaction is monitored by the appearance of I_2Br^- at 428 or 440 nm. These wavelengths avoid significant absorbance from small amounts of I_3^- (which has an intense absorption band at 353 nm) that also forms as shown by the proposed mechanism in eqs 15–18. Under these conditions the ratio of $[IBr_2^-]/[I_3^-]$

$$IBr_2^- \underset{k_{-1}}{\overset{k_1}{\rightleftharpoons}} IBr(aq) + Br^- \qquad (15)$$

$$IBr(aq) + I^- \underset{k_{-2}}{\overset{k_2}{\rightleftharpoons}} I_2Br^- \qquad (16)$$

$$I_2Br^- \underset{k_{-3}}{\overset{k_3}{\rightleftharpoons}} I_2(aq) + Br^- \qquad (17)$$

$$I_2(aq) + I^- \underset{k_{-4}}{\overset{k_4}{\rightleftharpoons}} I_3^- \qquad (18)$$

varies from 12 to 76 and the highest I_3^- concentration (6.4×10^{-7} M) does not contribute significantly to the absorbance at 428 or 440 nm. The rate expression is given by eq 19, on the basis of a preequilibrium condition for eq 15 and a rate-determining step given by eq 16. Table III gives the observed pseudo-first-order

$$\frac{-d[IBr]_T}{dt} = \frac{k_2[I^-][IBr]_T}{1 + ([Br^-]/K_1)} - k_{-2}[I_2Br^-] \qquad (19)$$

rate constants, k_r, measured by the PAF method. The k_r values are the sums of the forward and reverse rate constants defined by eqs 20 and 21. The slopes of the lines in Figure 4 give k_I values

$$k_r = k_I[I^-] + k_{II} \qquad (20)$$

$$k_I = \frac{k_2}{1 + ([Br^-]/K_1)} \qquad (21)$$

for three Br^- concentrations (0.60, 0.80, and 1.00 M). The intercepts in Figure 4 correspond to k_{II} values. Figure 5 is a plot of eq 21 where the intercept is zero and the slope gives $k_2 = (2.0 \pm 0.3) \times 10^9$ M^{-1} s^{-1}. The k_{-2} values differ slightly from the k_{II} values because small contributions of I_2(aq) and I_3^- to the final equilibrium mixture affect this reverse rate constant. Table IV summarizes the measured k_I and k_{II} values and gives the corrected k_{-2} rate constants. The average k_{-2} value for the data plotted in Figure 4 is 800 ± 300 s^{-1}. This is in good agreement with the calculated k_{-2} value of 1000 s^{-1} that results from $k_{-2} = k_2/K_2$. (The value of $K_2 = 2 \times 10^6$ M^{-1} is obtained from the work of Guidelli and Pergola[37] after corrections are made for the values of K_1 and K_3 given in Table I.) Hence, the PAF method can be used to study reversible kinetics.

The rate constants for eq 16 also can be measured by following the appearance of I_3^- at 353 nm since I_3^- is in rapid equilibrium with I_2Br^- via I_2(aq). Tables III and IV give two sets of conditions for these measurements. When Br^- is 1.00 M, the resulting k_2 value for the I_3^- indicator method is within the experimental error of the k_2 value determined from direct monitoring of IBr_2^-. Similarly, the two k_{-2} values in Table IV for 1.00 M Br^- fall within experimental error of each other, but the uncertainty of k_{-2} is larger for the I_3^- indicator method. When $[Br^-]$ is 0.10 M, a much higher concentration of I_3^- forms, and it is difficult to evaluate the k_{-2} rate constant. However, the k_I value falls on the line in Figure 5 and is used in the evaluation of k_2. The fact that I_3^- can be used to monitor the reaction indicates that $k_{-3}[Br^-] \gg k_4[I^-]$ and therefore $k_{-3} > 4 \times 10^8$ M^{-1} s^{-1} and $k_3 > 3 \times 10^7$ s^{-1}. We expect k_{-3} to be very large and similar in magnitude to k_4 (6×10^9 M^{-1} s^{-1}).

In order for eq 15 to be in rapid equilibrium prior to the rate-determining step in eq 16, the inequality $k_{-1}[Br^-] \gg k_2[I^-]$ must hold. Since the minimum Br^- concentration is 0.1 M and the maximum I^- concentration is 1.0×10^{-3} M, it follows that $k_{-1} \gg 2 \times 10^7$ M^{-1} s^{-1}. We would not expect k_{-1} to be larger than k_2, so the k_{-1} value should fall between 10^8 and 10^9 M^{-1} s^{-1}.

Comparison of Rate Constants. The relative values of the rate constants for the reactions with I^- are ICl(aq) < IBr(aq) < I_2(aq) as seen in Table V. The greater the degree of hydration of the interhalogen (IX), the less reactive it is with I^-. The hydration energies ($\Delta G°_{hydr}$, kJ mol^{-1}) for IX(g) + $H_2O \rightarrow$ IX(aq) are −9.28 (ICl), −7.62 (IBr), and −2.94 (I_2).[38] Two forms of iodine monochloride have been proposed to be in rapid equilibrium in aqueous solution.[1] The specifically hydrated form, H_2OICl, has an expanded iodine coordination (similar to ICl_2^-). Aside from proton-transfer processes, it does not react directly with other nucleophiles. The less hydrated form, ICl, reacts very rapidly (diffusion-controlled rate constants) with bases and constitutes 18% of ICl(aq).[1] We propose that IBr(aq) also exists as a mixture of H_2OIBr (structure **1**) and IBr. Solvent association has been

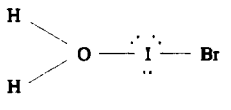

1

observed in spectral shift studies by Gillam.[28] There are marked shifts in the visible spectra of ICl and IBr and a smaller, but significant, shift in the I_2 spectrum as polar solvent is introduced (CCl_4 with variable amounts of ethanol). These changes are attributed to association of the polar solvent with the halogen species.

If we assume that I^- reacts with IBr at the diffusion limit (7×10^9 M^{-1} s^{-1}) and does not react directly with H_2OIBr, then the observed rate constant for IBr(aq) of 2.0×10^9 M^{-1} s^{-1} would correspond to a mixture of 29% IBr and 71% H_2OIBr. It is also possible to estimate the equilibrium constant, $K = [H_2OIBr]/[IBr] = 2.3$, from the free energies of hydration of IBr(g) and ICl(g). This estimate is based on the approximation that the solvation energies of the two interhalogen gases differ only by the relative ratio of $[H_2OIX]/[IX]$. This estimated equilibrium constant corresponds to 70% H_2OIBr and 30% IBr.

Table V also compares the dissociation rate constants for the reaction $I_2X^- \rightarrow I^-$ + IX(aq). The values increase enormously from 0.7 s^{-1} for I_2Cl^- to 800 s^{-1} for I_2Br^- to 8.5×10^6 s^{-1} for I_3^-. This reflects the relative stabilities of I_2X^- in regard to the unfavorable dissociation.

Determination of the Equilibrium Constant for the Hydrolysis of IBr_2^-. Acidic solutions of IBr_2^- with excess Br^- are reacted with NaH_2PO_4/Na_2HPO_4 buffer solutions in a Durrum stopped-flow spectrophotometer to give mixtures that vary in p[H^+] from 4.00

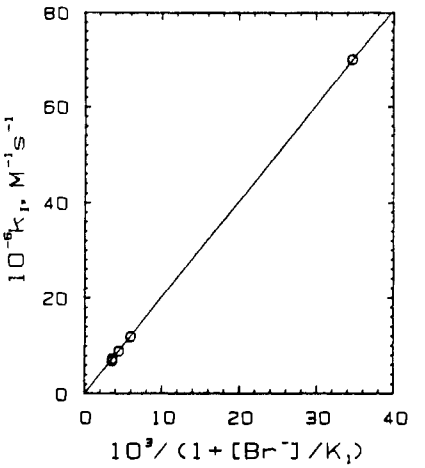

Figure 5. Bromide ion dependence of the second-order rate constants (k_I) for the reaction of IBr + I^- in 1.0 M H^+.

Table IV. Rate Constants, k_I and k_{II}, for the Reaction of IBr_2^- + I^- in 1.0 M H^+ at 25.0 °C

$[Br^-]$, M	$10^{-6}k_I$, M^{-1} s^{-1}	k_{II}, s^{-1}	k_{-2}, s^{-1}
1.00	6.8 (5)	900 (400)	1000 (400)
1.00	7.2 (5)[a]	1500 (600)	1700 (600)
0.80	8.9 (1)	470 (80)	500 (90)
0.60	11.9 (5)	800 (200)	900 (200)
0.10	70 (2)[a]	*b*	

[a] Measured by the appearance of I_3^- at 353 nm. [b] Not determined.

Table V. Comparison of Rate Constants for Interhalogen and Iodine Species[a]

ICl(aq) + $I^- \underset{k_{-a}}{\overset{k_a}{\rightleftharpoons}}$ I_2Cl^-	$k_a = 5.1 \times 10^8$ M^{-1} s^{-1} [b] $k_{-a} = 0.7$ s^{-1} [b] $K_a = 7.3 \times 10^8$ M^{-1}
IBr(aq) + $I^- \underset{k_{-2}}{\overset{k_2}{\rightleftharpoons}}$ I_2Br^-	$k_2 = 2.0 \times 10^9$ M^{-1} s^{-1} [c] $k_{-2} = 800$ s^{-1} [c] $K_2 = 3 \times 10^6$ M^{-1}
I_2(aq) + $I^- \underset{k_{-4}}{\overset{k_4}{\rightleftharpoons}}$ I_3^-	$k_4 = 6.2 \times 10^9$ M^{-1} s^{-1} [d,e] $k_{-4} = 8.5 \times 10^6$ s^{-1} [d,e] $K_4 = 7.3 \times 10^2$ M^{-1}

[a] 25.0 °C. [b] References 1 and 9 (μ = 1.0 M). [c] This work (μ = 1.0 M). [d] Turner, D. H.; Flyn, G. W.; Sutin, N.; Beitz, J. V. *J. Am. Chem. Soc.* **1972**, *94*, 1554–1559 (μ = 0.02 M). [e] Ruasse, M.-F.; Aubard, J.; Galland, B.; Adenier, A. *J. Phys. Chem.* **1986**, *90*, 4382–4388 (μ is low, but unspecified; $k_4 = 5.6 \times 10^9$ M^{-1} s^{-1}; $k_{-4} = 7.5 \times 10^6$ s^{-1}).

(37) Guidelli, R.; Pergola, F. *J. Inorg. Nucl. Chem.* **1969**, *31*, 1373–1381.
(38) Desideri, P. G.; Lepri, L.; Heimler, D. In *Standard Potentials in Aqueous Solution*; Bard, A. J., Parsons, R., Jordan, J., Eds.; Marcel Dekker: New York, 1985; pp 84–90.

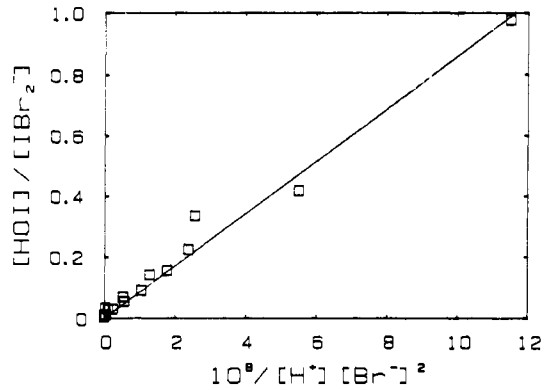

Figure 6. Determination of the equilibrium constant for the hydrolysis of IBr_2^- from spectrophotometric data at 375 nm. Slope = K_6 = (8.3 ± 0.3) × 10^{10} M^3.

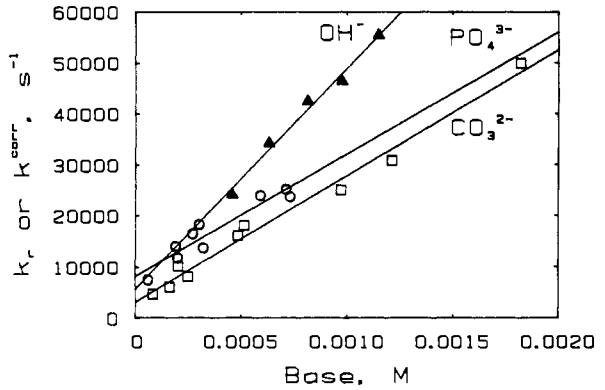

Figure 7. Pseudo-first-order rate constants vs base for the hydrolysis reaction of IBr(aq) ([IBr]$_T$ = 1.0 × 10^{-5} M; 253 nm, 25 °C; μ = 0.50 M (NaBr)): (▲) OH^-; (○) PO_4^{3-}; (□) CO_3^{2-}. The k^{cor} values are defined by eqs 28 and 29. The water hydrolysis rate constants (k_5) correspond to the intercepts × ([Br^-] + K_1)/K_1.

to 7.33 and in Br^- concentration from 0.10 to 0.30 M. The ionic strength is constant at 0.50 M(NaBr/$NaClO_4$), and the temperature is 25.0 °C. Stopped-flow mixing is used to obtain absorbance values at 375 nm after the hydrolysis reaction in eq 5 reaches equilibrium and before any disproportionation of HOI can occur.[39,40] (The molar absorptivities of IBr_2^- and IBr(aq) are 580 and 370 M^{-1} cm^{-1}, respectively, at 375 nm. A value of ϵ_{HOI} = 25 M^{-1} cm^{-1} at 375 nm is evaluated from the spectrum of HOI reported by Paquette and Ford.[41]) These data permit the determination of the equilibrium constant for IBr_2^- hydrolysis (K_6) in eq 22. The linear plot of [HOI]/[IBr_2^-] against 1/

$$K_6 = K_1K_5 = \frac{[HOI][H^+][Br^-]^2}{[IBr_2^-]} \qquad (22)$$

([H^+][Br^-]^2) in Figure 6 gives a value of (8.3 ± 0.3) × 10^{-10} M^3 for K_6. This gives a hydrolysis constant (K_5) for IBr(aq) equal to (2.4 ± 0.4) × 10^{-7} M^2, on the basis of K_1 = (3.5 ± 0.6) × 10^{-3} M at μ = 0.50. (Examination of Faull's data[3] shows only a 3% decrease in the value of K_1 as the ionic strength changes from 1.0 to 0.1 M.)

Kinetics of Base Hydrolysis of Iodine Monobromide. When IBr_2^- is added to base, the observed reaction is consistent with the mechanism in eqs 23–25. The rate of hydrolysis of IBr(aq)

$$IBr_2^- \rightleftarrows IBr(aq) + Br^- \quad K_1 \qquad (23)$$

$$IBr(aq) + H_2O \xrightarrow{k_5} HOI + Br^- + H^+ \qquad (24)$$

$$IBr(aq) + OH^- \xrightarrow{k_6} HOI + Br^- \qquad (25)$$

(39) Wren, J. C.; Paquette, J.; Sunder, S.; Ford, B. L. *Can. J. Chem.* **1986**, *64*, 2284–2296.
(40) Thomas, T. R.; Pence, D. T.; Hasty, R. A. *J. Inorg. Nucl. Chem.* **1980**, *42*, 183–186.
(41) Paquette, J.; Ford, B. L. *Can. J. Chem.* **1985**, *63*, 2444–2448.

Table VI. Pseudo-First-Order Rate Constants for the Hydrolysis Reaction of IBr(aq) with OH^-, CO_3^{2-}, and PO_4^{3-} [a]

[Br^-], M	10^3[OH^-], M	$10^{-4}k_r$, s^{-1}
0.500	0.457	2.4 (1)
0.500	0.631	3.4 (2)
0.500	0.813	4.2 (4)
0.500	0.977	4.6 (4)
0.500	1.148	5.5 (4)
0.500	0.500	3.3 (1)
0.400	0.500	3.8 (3)
0.300	0.500	5.1 (4)
0.200	0.500	6.8 (4)
0.100	0.500	14.0 (9)
B = CO_3^{2-}, [Br^-] = 0.500 M		
10^3[CO_3^{2-}], M	10^3[OH^-], M	$10^{-4}k^{cor}$,[b] s^{-1}
0.970	0.0457	2.51 (7)
0.249	0.0316	0.82 (2)
0.082	0.0186	0.47 (1)
1.821	0.1481	5.00 (8)
0.512	0.1001	1.81 (4)
0.202	0.0646	1.02 (2)
1.213	0.1412	3.10 (7)
0.483	0.0891	1.61 (2)
0.162	0.0457	0.612 (4)
B = PO_4^{3-} M, [Br^-] = 0.500 M		
10^3[PO_4^{3-}], M	10^3[OH^-], M	$10^{-4}k^{cor}$,[c] s^{-1}
0.591	1.023	2.4 (1)
0.274	0.933	1.65 (6)
0.058	0.550	0.74 (3)
0.733	1.349	2.37 (8)
0.318	1.122	1.37 (4)
0.197	1.023	1.17 (2)
0.708	1.288	2.51 (7)
0.301	1.047	1.82 (5)
0.193	1.000	1.40 (2)

[a] Conditions: [IBr]$_T$ = 1.0 × 10^{-5} M, λ = 253 nm, μ = 0.50 M (NaBr/$NaClO_4$). [b] $k^{cor} = k_r - k_6[OH^-]K_1/([Br^-] + K_1)$. [c] $k^{cor} = k_r - (k_6[OH^-] + k_B[CO_3^{2-}])K_1/([Br^-] + K_1)$.

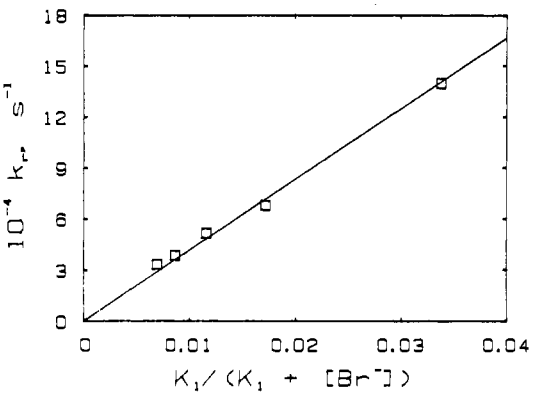

Figure 8. Effect of Br^- concentration on the hydrolysis rate constants for IBr_2^- with OH^-.

increases rapidly as the [OH^-] is increased. At 0.50 M Br^-, as [OH^-] increases from 0.46 to 1.15 mM, the k_r values increase from 24 000 to 55 000 s^{-1} (Table VI). A linear fit of k_r vs [OH^-] is given in Figure 7, where the intercept is (6 ± 3) × 10^3 s^{-1} and the slope is (4.2 ± 0.3) × 10^7 M^{-1} s^{-1}. The proposed mechanism involves Br^- suppression through the IBr_2^- equilibrium followed by hydrolysis of IBr(aq) by H_2O and by reaction with OH^- (eq 26). Therefore, the rate constant for the reaction of IBr(aq) +

$$k_r = \frac{(k_5 + k_6[OH^-])K_1}{[Br^-] + K_1} \qquad (26)$$

OH^- (k_6) can be calculated from the slope and gives k_6 = (6.0 ± 0.4) × 10^9 M^{-1} s^{-1}. The hydrolysis rate constant (k_5) is obtained from the intercept and gives k_5 = (9 ± 4) × 10^5 s^{-1}. Variation of the Br^- concentration at constant [OH^-] = 0.00050 M confirms

Scheme I. Pathways for the Hydrolysis of IBr with H_2O, OH^-, and Other Bases (B^-)

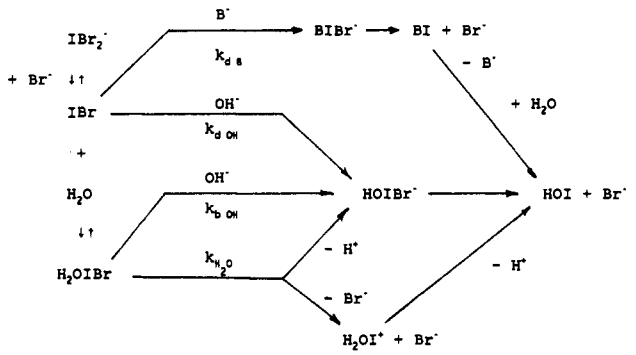

the dependence of k_r given in eq 26 (Table VI). Figure 8 shows values of k_r as a function of $K_1/(K_1 + [Br^-])$, where the slope = $k_5 + k_6[OH^-] = (4.16 \pm 0.09) \times 10^6\ s^{-1}$. This gives $k_6 = (6.5 \pm 0.2) \times 10^9\ M^{-1}\ s^{-1}$, which is within the experimental error of the value from Figure 7.

Effect of Carbonate and Phosphate Concentrations on the Kinetics of IBr(aq) Hydrolysis. The observed rate constants for the hydrolysis of IBr_2^- at constant Br^- concentration increase as the concentrations of CO_3^{2-} and PO_4^{3-} increase (Table VI). The general expression for the rate constant in the presence of bases (B) is given in eq 27. A corrected rate constant defined in eq

$$k_r = \frac{(k_5 + k_6[OH^-] + k_B[B])K_1}{[Br^-] + K_1} \quad (27)$$

28 is plotted against $[CO_3^{2-}]$ in Figure 7. The basic phosphate

$$k^{cor} = k_r - \frac{k_6[OH^-]K_1}{[Br^-] + K_1} = \frac{(k_5 + k_B[CO_3^{2-}])K_1}{[Br^-] + K_1} \quad (28)$$

solutions contained small amounts of carbonate, so the corrected rate constants obtained from eq 29 are plotted in Figure 7 for $[PO_4^{3-}]$.

$$k^{cor} = k_r - \frac{(k_6[OH^-] + k_B[CO_3^{2-}])K_1}{[Br^-] + K_1} = \frac{(k_5 + k_B[PO_4^{3-}])K_1}{[Br^-] + K_1} \quad (29)$$

The hydrolysis rate constants depend on the concentrations of CO_3^{2-} and PO_4^{3-}, but do not depend on the HCO_3^- or HPO_4^{2-} concentrations. The values of k_B are $(3.5 \pm 0.2) \times 10^9\ M^{-1}\ s^{-1}$ for CO_3^{2-} and $(3.5 \pm 0.4) \times 10^9\ M^{-1}\ s^{-1}$ for PO_4^{3-}. Despite the difference in the base strengths of PO_4^{3-} and CO_3^{2-} (the pK_a values for their conjugate acids are 11.34 and 9.70), both bases have the same rate constant for their reaction with IBr(aq). Although IBr(aq) is not selective in its reactions with CO_3^{2-} and PO_4^{3-}, it does not react with HCO_3^- or HPO_4^{2-}. This is in contrast to the behavior of ICl(aq), which has the same rate constant for reactions with $H_2PO_4^-$, HPO_4^{2-}, HCO_3^-, and CO_3^{2-}. Thus, IBr is much more selective in its reaction with bases than is ICl, as would be expected for a weaker Lewis acid.

The intercepts in Figure 7 are used to evaluate the water hydrolysis rate constant (k_5, s^{-1}) from the carbonate studies ($(4.6 \pm 1.4) \times 10^5$) and the phosphate studies ($(11.7 \pm 4.4) \times 10^5$), as well as from the hydroxide ion studies ($(9 \pm 4) \times 10^5$). The average k_5 value is $(8 \pm 3) \times 10^5\ s^{-1}$.

The proposed mechanism for the hydrolysis of IBr(aq) in Scheme I parallels the mechanism proposed for ICl(aq).[1] We propose that IBr(aq) consists of two species in rapid equilibrium. One form is H_2OIBr, with specific hydration by a water molecule at iodine (structure **1**) to give an adduct with 10 valence electrons around iodine which is similar to the structure for IBr_2^- (structure **2**). The other form of IBr(aq) is the less hydrated IBr molecule.

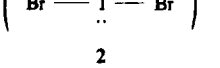

2

Table VII. Hydrolysis Rate Constants for Interhalogens[a] and Halogens[b]

reaction	rate constant	ref
$ICl(aq) + H_2O \rightarrow HOI + H^+ + Cl^-$	$2.4 \times 10^6\ s^{-1}$	1
$ICl(aq) + OH^- \rightarrow HOI + Cl^-$	$4.5 \times 10^9\ M^{-1}\ s^{-1}$	1
$ICl(aq) + B^- \rightarrow HOI + Cl^- + B^-$	$1.3 \times 10^9\ M^{-1}\ s^{-1}$	1
$IBr(aq) + H_2O \rightarrow HOI + H^+ + Br^-$	$8 \times 10^5\ s^{-1}$	c
$IBr(aq) + OH^- \rightarrow HOI + Br^-$	$6.0 \times 10^9\ M^{-1}\ s^{-1}$	c
$IBr(aq) + B^- \rightarrow HOI + Br^- + B^-$	$3.5 \times 10^9\ M^{-1}\ s^{-1}$	c
$I_2(aq) + H_2O \rightarrow HOI + H^+ + I^-$	$3.0\ s^{-1}$	2
$Br_2(aq) + H_2O \rightarrow HOBr + H^+ + Br^-$	$110\ s^{-1}$	2
$Cl_2(aq) + H_2O \rightarrow HOCl + H^+ + Cl^-$	$11.0\ s^{-1}$	2

[a] 25.0 °C. [b] 20 °C. [c] This work.

We propose that the latter form reacts at the diffusion-controlled rate constant ($7 \times 10^9\ M^{-1}\ s^{-1}$) with CO_3^{2-} and with PO_4^{3-} to give the intermediate species in structures **3** and **4**. As a result there

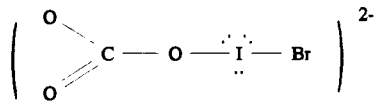

3

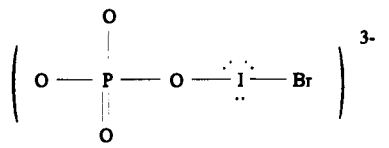

4

is no selectivity in regard to their relative base strengths. The H_2OIBr form is by comparison unreactive with these bases and the ratio $[IBr]/[IBr(aq)]$ equals $(3.5 \times 10^9)/(7 \times 10^9) = 0.5$. Therefore, we estimate that IBr(aq) is 50% IBr and 50% H_2OIBr.

The value for k_{OH} is larger than k_B, because OH^- is such a strong base that it can also react by proton transfer with H_2OIBr to give $HOIBr^-$ as shown in Scheme I. The hydroxide ion path depends on the diffusion-controlled rate constant with IBr ($k_{d\,OH}$) and the proton-transfer rate constant with H_2OIBr($k_{b\,OH}$). The combination of these two paths gives eq 30. The $k_{b\,OH}$ value is

$$k_{OH} = k_{d\,OH}[IBr]/[IBr(aq)] + k_{b\,OH}[H_2OIBr]/[IBr(aq)] \quad (30)$$

difficult to evaluate, but was estimated to be about $4 \times 10^9\ M^{-1}\ s^{-1}$ for H_2OICl[1] and apparently has a similar value for H_2OIBr.

Hydration of IBr. The rate constants for the reaction of CO_3^{2-} and PO_4^{3-} with IBr(aq) permit evaluation of its composition as 50% IBr and 50% H_2OIBr. Similar assumptions for the rate constant of IBr(aq) with I^- relative to the diffusion limit give 29% IBr and 71% H_2OIBr. On the other hand, the relative rate constants for ICl(aq) and IBr(aq) would indicate that if ICl(aq) is 18% ICl,[1] then IBr(aq) must be 70% IBr and 30% H_2OIBr. The estimate based on relative solution energies of IBr(g) and ICl(g) relative to the percent H_2OICl gives 30% IBr and 70% H_2OIBr. The average of these four estimates is 45% IBr and 55% H_2OIBr. Since buffer rate constants were used to evaluate the composition of ICl(aq),[1] we also select the CO_3^{2-} and PO_4^{3-} rate constants to be the best estimate of the composition of IBr(aq) to be $[H_2OIBr]/[IBr] = 50/50 = 1.0$.

Conclusions

The hydrolysis rate constants (s^{-1}) decrease from 2.4×10^6 for ICl(aq) to 9×10^5 for IBr(aq) and to 3.0 for I_2(aq) (Table VII). Since iodine is nonpolar, it will exist predominantly as I_2 rather than as H_2OI_2. In addition, the loss of I^- is less favorable than Br^- or Cl^- in terms of the solvation of the anions. Hence, the I_2(aq) hydrolysis rate constant is many orders of magnitude smaller than those of ICl(aq) and IBr(aq). The gaseous halogen–halogen bond strengths (kJ mol^{-1})[42] are ICl (211.3) > IBr (177.8) > I_2 (151.0),

(42) Darwent, deB. B. *Natl. Stand. Ref. Data Ser. (U.S. Natl. Bur. Stand.)* **1970**, *31*, 33.

which would predict relative k_{H_2O} values in the opposite order than is seen. Instead, the relative k_{H_2O} values follow the trend given by the dipole moments[43] for ICl (1.24) > IBr (0.72) > I_2 (0.00). This shows the importance of aquation.

The reactions of IBr_2^- with I^-, with OH^-, and with water parallel the behavior of ICl_2^-. The reactive species with I^- is IBr, while both H_2OIBr and IBr can react with OH^-. The degree of specific H_2O coordination of IBr(aq) (to form H_2OIBr) is less than for ICl(aq). Our best estimate gives 50% H_2OIBr and 50% IBr. The uncertainty is large, but the I^- and base rate constants indicate a lower degree of specific water coordination for IBr. This is consistent with a smaller dipole moment for IBr compared to ICl. Nevertheless, the hydrolysis rate constant for IBr(aq) is 3×10^4 to 6×10^2 larger than previous estimates.[4,5]

This work also shows that the PAF technique can be used to measure very rapid reversible as well as irreversible kinetics.

Acknowledgment. This work was supported by National Science Foundation Grants CHE-8720318 and CHE-9024291.

Registry No. IBr, 7789-33-5; I^-, 20461-54-5.

(43) Lovas, F. J.; Tiemann, E. *J. Phys. Chem. Ref. Data* **1974**, *3*, 609.

Contribution from the Department of Chemistry, Purdue University, West Lafayette, Indiana 47907

Non-Metal Redox Kinetics: A Reexamination of the Mechanism of the Reaction between Hypochlorite and Nitrite Ions

Debra W. Johnson and Dale W. Margerum*

Received June 25, 1991

Hypochlorite oxidation of NO_2^- does not take place by oxygen atom transfer, but proceeds by Cl^+ transfer from HOCl to NO_2^- to give NO_2Cl as a reaction intermediate. The kinetics indicate that the subsequent decomposition of NO_2Cl proceeds by two pathways: loss of Cl^- to give NO_2^+ and reaction of NO_2Cl with NO_2^- to form N_2O_4 and Cl^-. At high Cl^- and low OH^- and NO_2^- concentrations the overall rate of NO_3^- formation is suppressed by Cl^-. The relative reactivities for the reaction with NO_2^+ are $OH^- \gg Cl^- \gg H_2O$. Although oxygen isotope experiments are consistent with a Cl^+ transfer mechanism, the rate of exchange of oxygen between OCl^- and H_2O is relatively rapid (even at high pH in the absence of Cl^-). We predict that the OCl^-/H_2O exchange rate in base will be independent of OH^- concentration.

Introduction

The reaction between hypochlorite ion and nitrite ion (eq 1) has long been one of the classic examples of an oxygen atom

$$OCl^- + NO_2^- \rightarrow Cl^- + NO_3^- \quad (1)$$

transfer process,[1] and it is still a frequently used textbook example.[2] This is based on the work of Anbar and Taube,[1] who reported that ^{18}O was completely transferred from $^{18}OCl^-$ to give labeled nitrate.

In recent years Margerum and co-workers[3-7] have studied a series of much more rapid redox reactions of hypochlorite, where the overall stoichiometry gives the appearance of oxygen atom transfer (eqs 2-5). All four of these reactions are acid-catalyzed,

$$OCl^- + I^- \rightarrow OI^- + Cl^- \quad (2)$$

$$OCl^- + Br^- \rightarrow OBr^- + Cl^- \quad (3)$$

$$OCl^- + SO_3^{2-} \rightarrow SO_4^{2-} + Cl^- \quad (4)$$

$$OCl^- + CN^- \rightarrow OCN^- + Cl^- \quad (5)$$

and in each case HOCl is many orders of magnitude more reactive than OCl^-. Direct evidence is found for Cl^+ transfer rather than O atom transfer in the reactions with sulfite[8] and with cyanide.[7]

The kinetics and mechanisms in each case indicate nucleophilic attack at chlorine rather than at oxygen to give the initial products in eqs 6-9. Subsequent hydrolysis reactions occur (eqs 10-13)

$$HOCl + I^- \rightarrow ICl + OH^- \quad (6)$$

$$HOCl + Br^- \rightarrow BrCl + OH^- \quad (7)$$

$$HOCl + SO_3^{2-} \rightarrow ClSO_3^- + OH^- \quad (8)$$

$$HOCl + CN^- \rightarrow ClCN + OH^- \quad (9)$$

$$ICl + 2OH^- \rightarrow OI^- + Cl^- + H_2O \quad (10)$$

$$BrCl + 2OH^- \rightarrow OBr^- + Cl^- + H_2O \quad (11)$$

$$ClSO_3^- + H_2O \rightarrow SO_4^{2-} + Cl^- + 2H^+ \quad (12)$$

$$ClCN + 2OH^- \rightarrow OCN^- + Cl^- + H_2O \quad (13)$$

to give the product stoichiometry in eqs 2-5. The kinetics of hydrolysis have been determined for ICl,[9] $ClSO_3^-$,[8] and ClCN.[10]

The question as to why NO_2^- should behave so differently than other nucleophiles prompted us to reexamine the OCl^-/NO_2^- reaction. A simple rate expression (eq 14) is expected from the

$$\frac{-d[OCl^-]}{dt} = k[NO_2^-][OCl^-] \quad (14)$$

Anbar and Taube[1] mechanism. They did not determine the actual rate expression, but they discussed the possibility that the activated complexes might also include the following two structures:

(1) Anbar, M.; Taube, H. *J. Am. Chem. Soc.* **1958**, *80*, 1073-1077.
(2) (a) Shriver, D. F.; Atkins, P. W.; Langford, C. H. *Inorganic Chemistry*; Freeman: New York, 1990; p 241. (b) Purcell, K. F.; Kotz, J. C. *Inorganic Chemistry*; Saunders: Philadelphia, PA, 1977; pp 656-657. (c) Jolly, W. L. *Modern Inorganic Chemistry*, 2nd ed.; McGraw-Hill: New York, 1991; p 184.
(3) Kumar, K.; Day, R. A.; Margerum, D. W. *Inorg. Chem.* **1986**, *25*, 4344-4350.
(4) Nagy, J. C.; Kumar, K.; Margerum, D. W. *Inorg. Chem.* **1988**, *27*, 2773-2780.
(5) Kumar, K.; Margerum, D. W. *Inorg. Chem.* **1987**, *26*, 2706-2711.
(6) Fogelman, K. D.; Walker, D. M.; Margerum, D. W. *Inorg. Chem.* **1989**, *28*, 986-993.
(7) Gerritsen, C. M.; Margerum, D. W. *Inorg. Chem.* **1990**, *29*, 2757-2762.
(8) Yiin, B. S.; Margerum, D. W. *Inorg. Chem.* **1988**, *27*, 1670-1672.
(9) Wang, Y. L.; Nagy, J. C.; Margerum, D. W. *J. Am. Chem. Soc.* **1989**, *111*, 7838-7844.
(10) Bailey, P. L.; Bishop, E. *J. Chem. Soc., Dalton Trans.* **1973**, *9*, 912-916.

0020-1669/91/1330-4845$02.50/0